

Temperature dependence of spin-split peaks in transverse electron focusing

Chengyu Yan,^{1,2, a)} Sanjeev Kumar,^{1,2} Michael Pepper,^{1,2} Patrick See,³ Ian Farrer,^{4, b)} David Ritchie,⁴ Jonathan Griffiths,⁴ and Geraint Jones⁴

¹⁾London Centre for Nanotechnology, 17-19 Gordon Street, London WC1H 0AH, United Kingdom

²⁾Department of Electronic and Electrical Engineering, University College London, Torrington Place, London WC1E 7JE, United Kingdom

³⁾National Physical Laboratory, Hampton Road, Teddington, Middlesex TW11 0LW, United Kingdom

⁴⁾Cavendish Laboratory, J.J. Thomson Avenue, Cambridge CB3 0HE, United Kingdom

(Dated: 14 November 2018)

We present experimental results of transverse electron focusing measurements performed using n-type GaAs. In the presence of a small transverse magnetic field (B_{\perp}), electrons are focused from the injector to detector leading to focusing peaks periodic in B_{\perp} . We show that the odd-focusing peaks exhibit a split, where each sub-peak represents population of a particular spin branch emanating from the injector. The temperature dependence reveals the peak splitting is well defined at low temperature whereas it smears out at high temperature indicating the exchange-driven spin polarisation in the injector is dominant at low temperatures.

BACKGROUND

The electron transport through a quasi one-dimensional (1D) system realised using the two-dimensional electron gas (2DEG) formed at the interface of GaAs/AlGaAs heterostructure has been extensively studied. A 1D system provides an outstanding platform to envisage not only the non-interacting quantum mechanical system where the conductance quantisation¹⁻³ is in the units of $n \times \frac{2e^2}{h}$, where $n=1,2,3...$ are different 1D energy subbands, but also a venue to explore many-body physics⁴⁻⁹. Recently, the progress in the physics of many-body 1D system has gained momentum due to prediction and experimental demonstration of rich-phases in low-density 1D system leading to incipient Wigner crystallisation^{6,7,10}. Moreover the origin of the 0.7 conductance anomaly in the frame work of many-body 1D system is still debated¹¹⁻¹⁵. The 0.7 anomaly has two major features: first, in the presence of in-plane magnetic field, the 0.7 anomaly evolves into $0.5 \times \frac{2e^2}{h}$ plateau, which indicates it is spin-related⁴; second, the 0.7 anomaly was found to weaken (strengthen) with decreasing (increasing) temperature⁴. These remarkable observations have led to a volume of theoretical and experimental attempts to probe the intrinsic spin polarisation associated with the 0.7 anomaly, however there is no consensus as such on the origin of this anomaly¹¹⁻¹⁵. Therefore, to shed more light on the 0.7 anomaly, it is essential to perform a direct measurement on the spin polarisation within a 1D channel.

A scheme based on transverse electron focusing (TEF) was proposed to address the spin polarisation^{16,17}, and was validated in p-type GaAs^{18,19} and n-type InSb²⁰. Within this scheme, the spin polarisation can be extracted from the asymmetry of the two sub-peaks of the first focusing peak. Recently, we showed that injection of 1D electrons whose spins have been spatially separated, can be detected in the form of a split in the first focusing peak, where the two sub-peaks represent the population of detected spin states²¹. In the

^{a)}Electronic mail: uceeya3@ucl.ac.uk

^{b)}Currently at Department of Electronic and Electrical Engineering, University of Sheffield, Mappin Street, Sheffield S1 3JD, United Kingdom.

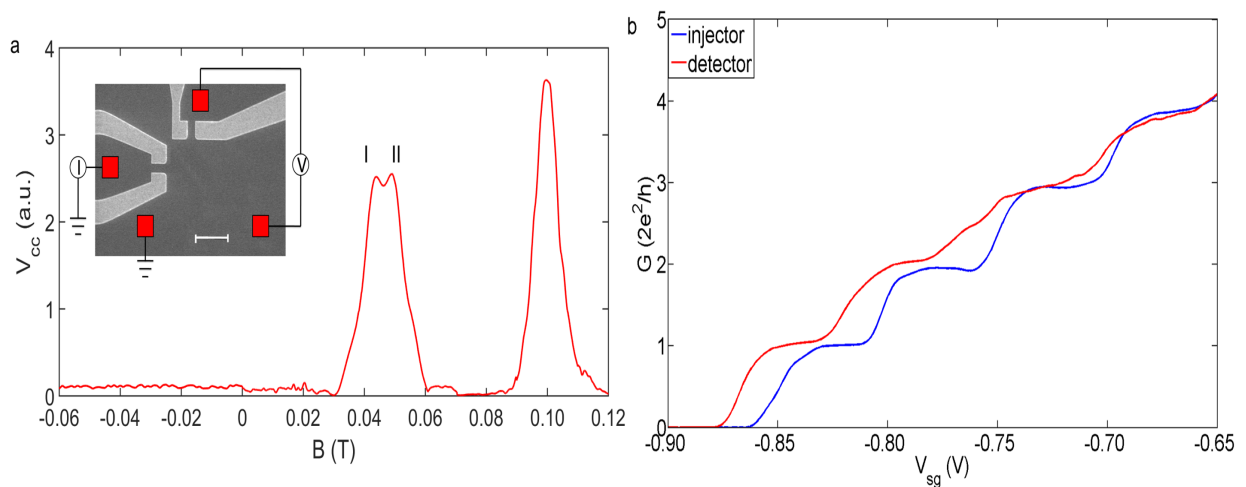


FIG. 1. **The experiment setup and device characteristic.** (a) A representative plot of transverse electron focusing with both the injector and detector set to G_0 ($2e^2/h$). V_{cc} is the voltage drop across the detector. Focusing peaks are well defined with positive magnetic field and the signal is negligible with negative magnetic field. The first peak shows pronounced splitting. The two sub-peaks have been highlighted as peak I and peak II. The inset shows an SEM image of the device. The separation between the injector and detector is $1.5 \mu\text{m}$. Red squares form the Ohmic contacts whereas two pairs of grey-coloured gates, left and top, form the injector and detector, respectively. The scale bar is $2 \mu\text{m}$. (b) Conductance characteristics of the injector and detector.

present work, we report the temperature dependence of spin-split first focusing peak, and analyse the results based on the spin-gap present between the two spin species.

METHOD

The devices studied in the present work were fabricated from the high mobility two dimensional electron gas (2DEG) formed at the interface of GaAs/ $\text{Al}_{0.33}\text{Ga}_{0.67}\text{As}$ heterostructure. At 1.5 K, the measured electron density (mobility) was $1.80 \times 10^{11} \text{cm}^{-2}$ ($2.17 \times 10^6 \text{cm}^2 \text{V}^{-1} \text{s}^{-1}$), therefore the mean free path is over $10 \mu\text{m}$ which is much larger than the electron propagation length. The experiments were performed in a cryofree dilution refrigerator with a lattice temperature of 20 mK using the standard lockin technique. The range of temperature dependence measurement was from 20 mK to 1.8 K.

RESULTS AND DISCUSSION

Figure 1(a) shows the experimental setup along with a typical focusing spectrum obtained using the device shown in the inset. The focusing device is specially designed so that the injector and detector can be controlled separately to avoid a possible cross-talking between them^{21–23}. The quantum wire used for the injector and detector has a width (confinement direction) of 500 nm and length (current flow direction) of 800 nm. Both the injector and detector show well defined conductance plateaus as shown in Fig. 1(b). Further details on the device are given in the caption of Fig. 1.

With negative magnetic field, the measured signal is almost zero because electrons bend into the opposite direction and thus miss the detector. It is also evident that the Shubnikov-de Haas oscillation and quantum Hall effect do not contribute to the observation. In the presence of a small positive transverse magnetic field B_{\perp} electrons are focused from the injector to detector leading to focusing peaks periodic in B_{\perp} while the detected signal is

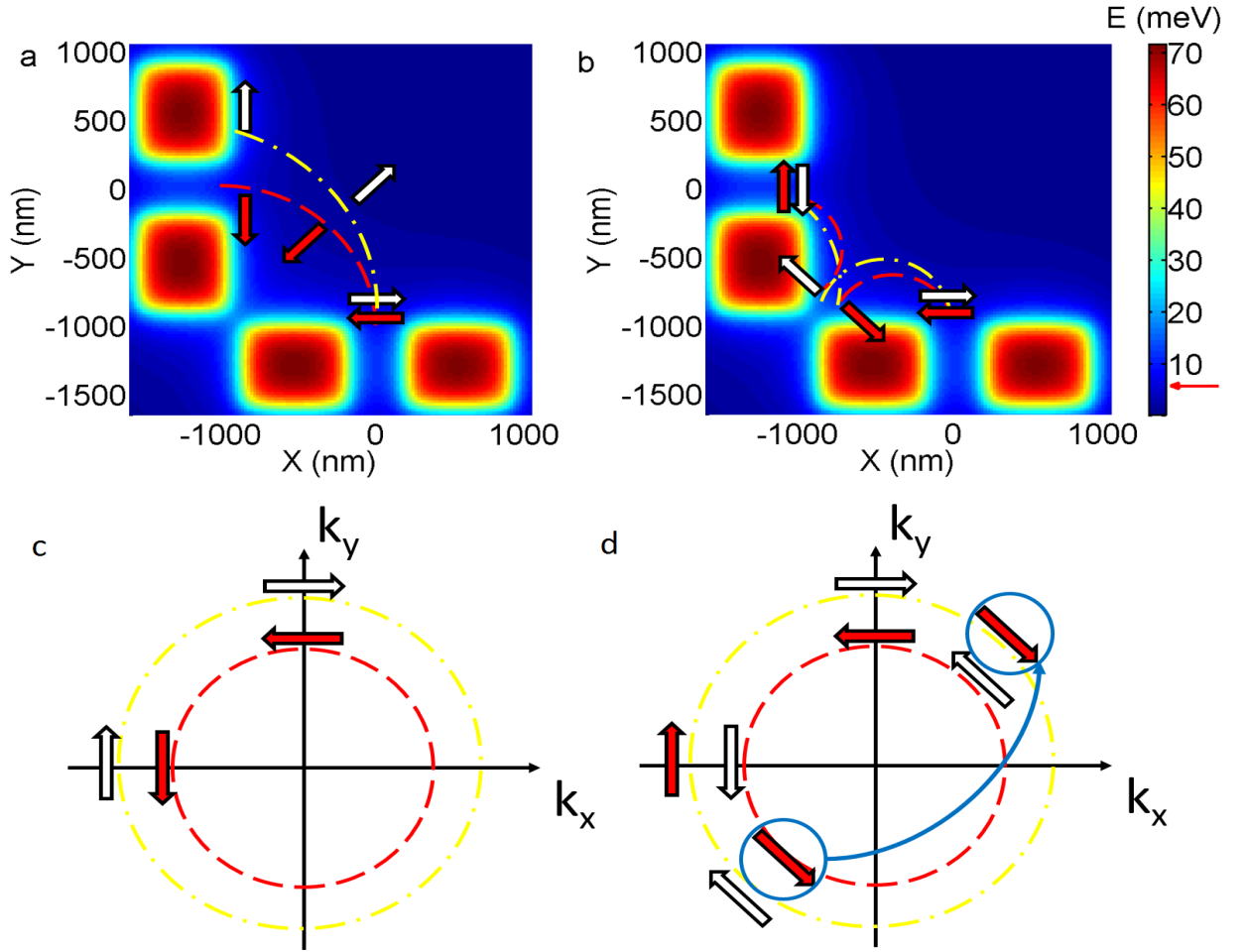


FIG. 2. **Mechanism of peak splitting.** (a)-(b) Peak splitting in the coordinate-space for first and second focusing peaks, respectively. The red and white arrows represent spin-up and spin-down electrons, the coloured blocks stand for the electrostatic potential and the red-dashed trace is with smaller cyclotron radius while the yellow-dotted one is with larger cyclotron radius. (c)-(d), Peak splitting in the k -space for first and second focusing peaks, respectively. The electrons travel from $(0, k_y)$ to $(-k_x, 0)$ anticlockwise in plot (c). In plot (d), the thick blue arrow highlights the transition after reflection at the boundary of electrostatic potential formed between the injector and detector.

negligible at the negative magnetic field end. The calculated periodicity of 60 mT using the relation²³,

$$B_{focus} = \frac{\sqrt{2}\hbar k_F}{eL} \quad (1)$$

is in good agreement with the experimental result. Here e is the elementary charge and \hbar is the reduced Planck constant, L is the separation between the injector and detector (in the 90° focusing device geometry, this is the separation along the diagonal direction). In addition to the periodic focussing peak which is a manifestation of the semi-classical electron cyclotron orbit, it is interesting to notice the splitting of odd-numbered focusing peaks. It is suggested that this anomalous splitting of odd-numbered focusing peaks arises from the spin-orbit interaction (SOI)^{16,17} and has been successfully observed in GaAs hole gas^{18,19} and InSb electron gas²⁰. We recently demonstrated splitting of odd-numbered focusing peaks in n-GaAs²¹ where a longer quantum wire possessing partially polarised

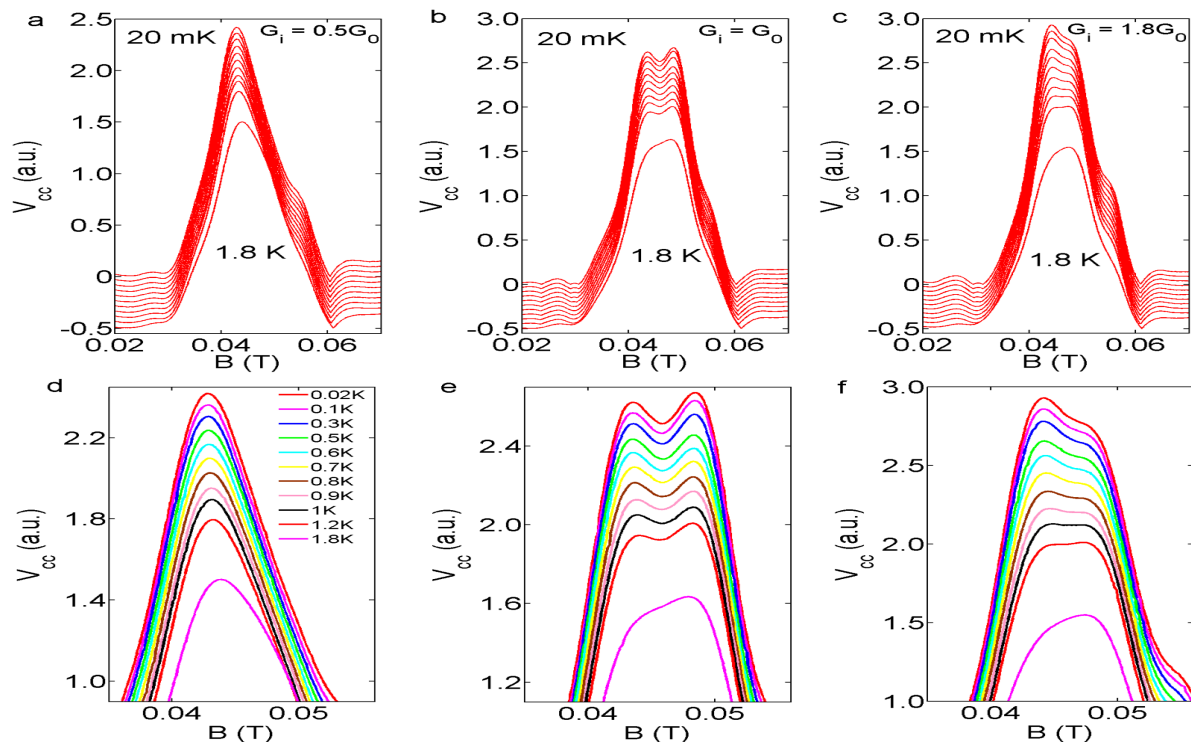


FIG. 3. **Temperature dependence of TEF.** (a)-(c) The injector was set to $0.5G_0$, G_0 and $1.8G_0$, respectively. The lattice temperature was incremented from 20 mK (top trace) to 1.8 K (bottom trace). Data have been offset vertically for clarity. (d)-(f), zoom-in of the data in (a)-(c).

and spatially separated 1D electrons was used to inject the polarised 1D electrons into the 2D regime and subsequently measured across the detector in the form of a split in the first focusing peak. Here we are interested in investigating the thermal effect on the spin states within the 1D channel via the transverse electron focusing. We note that the splitting smears out when the thermal energy $k_B T$ exceeds $2\Delta E$ (ΔE is the energy difference between the two spin branches) agreeing with the theoretical prediction¹⁷.

Before we discuss the temperature dependence effect, it is important to understand the mechanism responsible for the observed peak splitting. Figure 2(a) and (b) show the potential profile of the split gates forming the injector (bottom pair) and the detector (left pair). In the presence of SOI, the two spin species follow different cyclotron radii as shown in Fig. 2(a) thus resulting in two sub-peaks in the first focusing peak. However, the situation is different for the second focusing peak where a scattering at the boundary of electrostatic potential created by the split gates is involved as shown in Fig. 2(b). In this case, a spin-up electron (red arrow in the colourplots) initially follows a smaller cyclotron radius while it possesses a larger radius after the scattering^{16,17} and vice-versa for the spin-down electron (white arrow), thus the two spin species re-join at the detector. The underneath reasoning for the peak splitting can be found in the k-space in Fig. 2(c) and (d). Here we assume the spin-orbit interaction is of Rashba-type, however, the analysis holds valid for Dresselhaus effect in bulk as well. For the first focusing peak (Fig. 2(c)), the two spin-species travel from $(0, k_y)$ to $(-k_x, 0)$ along different Fermi surfaces. For the second focusing peak (Fig. 2(d)), the same argument holds true before the scattering, however, the momentum changes its sign while the spin orientation remains preserved after the scattering¹⁶. Therefore, a spin-up electron (red arrows) initially occupying the inner Fermi surface hops to the outer Fermi surface after the scattering to guarantee both the sign of the momentum and the spin orientation are in the correct order (the hopping is highlighted by the thick

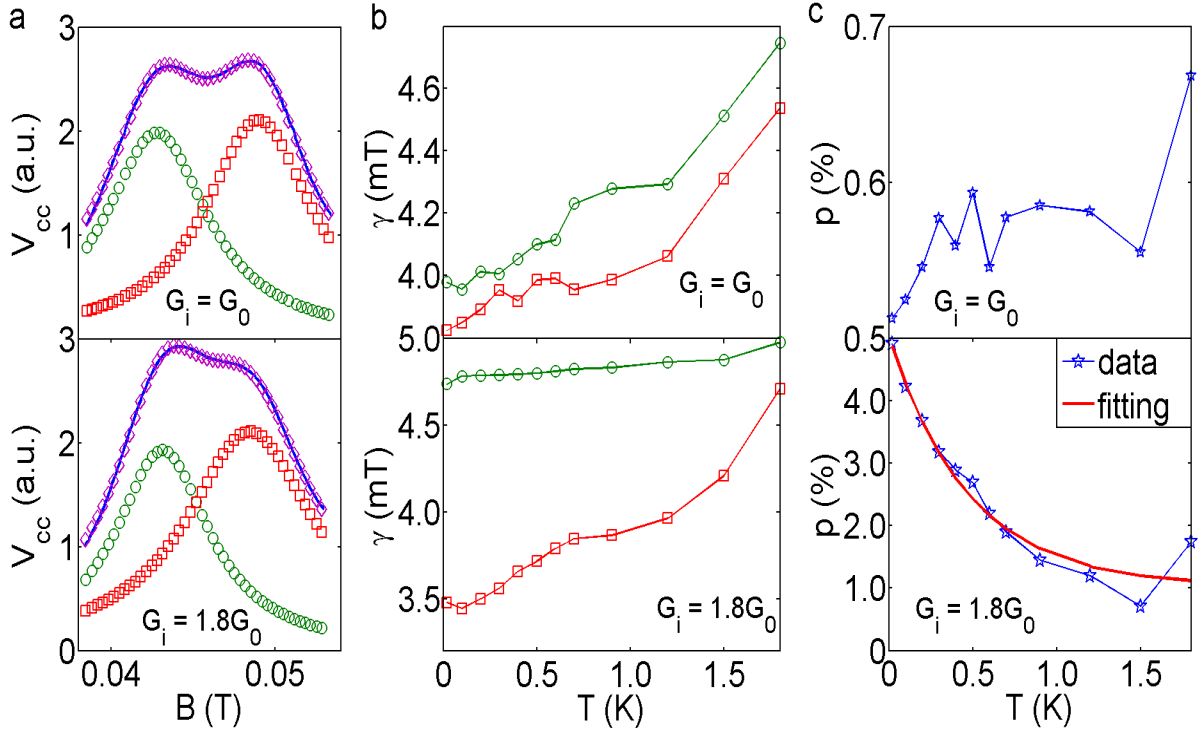


FIG. 4. **Analysis of the temperature dependence data.** (a) Reconstructing the first focusing peak with two Lorentzian peaks at 20 mK. The solid blue line is the experimental data, the green-round marker is the fit for peak I and red-square marker is the fit for peak II and the magenta-diamond marker highlights the reconstructed focusing peak. (b) FWHM, γ as a function of temperature; the sub-peaks broaden with increasing temperature in both cases. The markers represent the same meaning as in plot (a). (c) The polarisation measured with $G_i = G_0$ fluctuates around 0.6%. On the other hand, the polarisation measured with $G_i = 1.8G_0$ follows an exponential decay.

blue arrow in Fig. 2(d)) and vice-versa for the spin-down electron. The cyclotron radius is proportional to the momentum, so that the alternation in cyclotron radius occurs in the coordinate-space as a consequence of hopping between two Fermi surfaces which leads to a single second focusing peak.

Figure 3(a)-(c) show the temperature dependence of focusing results with injector set to $0.5G_0$, G_0 and $1.8G_0$, respectively, where the lattice temperature is incremented from 20 mK (the electron temperature is calibrated to be around 70 mK) to 1.8 K, and Fig. 3(d)-(f) shows the zoom-in of the data in Fig. 3(a)-(c), respectively. For $G_i = 0.5G_0$ (Fig. 3(a)) a single peak is observed (as only one spin-subband is occupied), which broadens gradually at higher temperature. In addition, the focusing peak shifts towards the center of the spectrum and becomes more symmetric at higher temperature (see the bottom trace, $T = 1.8$ K, Fig. 3(a) and (d)). This may be due to a possible electron transition between the two spin-subbands at relatively high temperature. In comparison, for $G_i = G_0$ (Fig. 3(b)) the sub-peaks, each representing a spin-state, are present from 20 mK up to 1.2 K. However, the dip in the first focusing peak leading to two sub-peaks smears out at 1.8 K (Fig. 3(b) and (e)). With G_i set to $1.8G_0$ (Fig. 3(c)), the splitting is not well resolved and the left sub-peak (I) dominates the spectrum. We note that on increasing the temperature the peak I gradually reduced in amplitude to result in an asymmetric first focusing peak at 1.8 K. In n-type InSb, the splitting was pronounced even at 10 K, which is consistent with the fact the peak splitting was around 60 mT, an indication of strong SOI in InSb²⁰, which is one

order larger than the peak splitting of 5.5 mT measured in the present case.

To extract the peak width and amplitude accurately considering the two sub-peaks may partially overlap with each other, we use two Lorentzian peaks to reconstruct the experimental data as shown in Fig. 4(a) using the relation,

$$A(B) = \sum_{i=1,2} A_i \times \frac{\gamma_i^2}{\gamma_i^2 + (B - B_i)^2} \quad (2)$$

where A_i is the amplitude of the peak i ($i=1, 2$ for peak I and peak II, respectively), γ_i denotes the full width at half maximum (FWHM), B_i is the center of the peak. Two noticeable results can be extracted from the fitting: First, it is seen from Fig. 4(b) that γ (see caption of Fig. 4 for details on traces and symbols representing peak I and peak II) for both peak I and peak II increases with rising temperature regardless of the injector conductance which indicates the thermal broadening of the sub-peaks prevents the observation of peak splitting at high temperature. It may be noted that peak I for $G_i = 1.8G_0$ is relatively robust against temperature compared to other peak (both peaks of G_0 and peak II of $1.8G_0$). Second, the measured spin polarization p ($p = |\frac{A_1 - A_2}{A_1 + A_2}|$) with $G_i = G_0$ fluctuates around 0.6% and shows no explicit temperature dependence which agrees with the fact that spin polarisation at conductance plateau should remain at 0 regardless of temperature (Fig. 4(c), upper plot). On the other hand, when G_i is set to $1.8G_0$, the extracted spin polarisation decays from 5% to 0.8% (Fig. 4(d), lower plot) following the relation¹⁵,

$$p = \alpha \exp\left(-\frac{k_B T}{\Delta E}\right) + c \quad (3)$$

where α is a prefactor accounting for the amplitude, k_B is the Boltzmann constant, ΔE is the energy difference between the two spin-branches and c accounts for the small residual value arises from the uncertainty in the experiment. We extracted the value of ΔE to be around 0.041 meV (corresponding to 0.5 K). The theory¹⁷ predicts the splitting should persist until $k_B T$ exceeds $2\Delta E$ (i.e. 1 K in our case) which agrees reasonably well with our result that the peak splitting is observable up to 1.2 K.

CONCLUSION

In conclusion, we showed the temperature dependence of the transverse electron focusing where the contribution of the two spin states manifested as two sub-peaks in the first focusing peak. It was observed that the peak splitting is well defined from 20 mK up to 1.2 K and beyond this temperature the peak splitting smeared out. Moreover, the focusing peak has a tendency to become more symmetric at higher temperature indicating a possible equilibrium between the two spin branches due to thermal excitation.

The work is funded by the Engineering and Physical Sciences Research Council (EPSRC), UK.

¹Thornton, T.J., Pepper, M., Ahmed, H., Andrews, D., Davies, G.J.: One-dimensional conduction in the 2D electron gas of a GaAs-AlGaAs heterojunction. *Phys. Rev. Lett.* **56**, 1198–1201 (1986). doi:10.1103/PhysRevLett.56.1198

²Wharam, D.A., Thornton, T.J., Newbury, R., Pepper, M., Ahmed, H., Frost, J.E.F., Hasko, D.G., Peacock, D.C., Ritchie, D.A., Jones, G.A.C.: One-dimensional transport and the quantisation of the ballistic resistance. *Journal of Physics C: Solid State Physics* **21**(8), 209 (1988)

³van Wees, B.J., van Houten, H., Beenakker, C.W.J., Williamson, J.G., Kouwenhoven, L.P., van der Marel, D., Foxon, C.T.: Quantized conductance of point contacts in a two-dimensional electron gas. *Phys. Rev. Lett.* **60**, 848–850 (1988). doi:10.1103/PhysRevLett.60.848

⁴Thomas, K.J., Nicholls, J.T., Simmons, M.Y., Pepper, M., Mace, D.R., Ritchie, D.A.: Possible spin polarization in a one-dimensional electron gas. *Phys. Rev. Lett.* **77**, 135–138 (1996). doi:10.1103/PhysRevLett.77.135

⁵Sfigakis, F., Ford, C.J.B., Pepper, M., Kataoka, M., Ritchie, D.A., Simmons, M.Y.: Kondo effect from a tunable bound state within a quantum wire. *Phys. Rev. Lett.* **100**, 026807 (2008). doi:10.1103/PhysRevLett.100.026807

- ⁶Hew, W.K., Thomas, K.J., Pepper, M., Farrer, I., Anderson, D., Jones, G.A.C., Ritchie, D.A.: Incipient formation of an electron lattice in a weakly confined quantum wire. *Phys. Rev. Lett.* **102**, 056804 (2009). doi:10.1103/PhysRevLett.102.056804
- ⁷Kumar, S., Thomas, K.J., Smith, L.W., Pepper, M., Creeth, G.L., Farrer, I., Ritchie, D., Jones, G., Griffiths, J.: Many-body effects in a quasi-one-dimensional electron gas. *Phys. Rev. B* **90**, 201304 (2014). doi:10.1103/PhysRevB.90.201304
- ⁸Yan, C., Kumar, S., Pepper, M., See, P., Farrer, I., Ritchie, D., Griffiths, J., Jones, G.: Fano resonance in a cavity-reflector hybrid system. *Phys. Rev. B* **95**, 041407 (2017). doi:10.1103/PhysRevB.95.041407
- ⁹Yan, C., Kumar, S., Pepper, M., See, P., Farrer, I., Ritchie, D., Griffiths, J., Jones, G.: Interference effects in a tunable quantum point contact integrated with an electronic cavity. *Phys. Rev. Applied* **8**, 024009 (2017). doi:10.1103/PhysRevApplied.8.024009
- ¹⁰Meyer, J.S., Matveev, K.A.: Wigner crystal physics in quantum wires. *Journal of Physics: Condensed Matter* **21**(2), 023203 (2009)
- ¹¹Wang, C.-K., Berggren, K.-F.: Spin splitting of subbands in quasi-one-dimensional electron quantum channels. *Phys. Rev. B* **54**, 14257–14260 (1996). doi:10.1103/PhysRevB.54.R14257
- ¹²Wang, C.-K., Berggren, K.-F.: Local spin polarization in ballistic quantum point contacts. *Phys. Rev. B* **57**, 4552–4556 (1998). doi:10.1103/PhysRevB.57.4552
- ¹³Reilly, D.J., Buehler, T.M., O'Brien, J.L., Hamilton, A.R., Dzurak, A.S., Clark, R.G., Kane, B.E., Pfeiffer, L.N., West, K.W.: Density-dependent spin polarization in ultra-low-disorder quantum wires. *Phys. Rev. Lett.* **89**, 246801 (2002). doi:10.1103/PhysRevLett.89.246801
- ¹⁴Reilly, D.J.: Phenomenological model for the 0.7 conductance feature in quantum wires. *Phys. Rev. B* **72**, 033309 (2005). doi:10.1103/PhysRevB.72.033309
- ¹⁵Bruus, H., Cheianov, V.V., Flensberg, K.: The anomalous 0.5 and 0.7 conductance plateaus in quantum point contacts. *Physica E: Low-dimensional Systems and Nanostructures* **10**(1), 97–102 (2001). doi:10.1016/S1386-9477(01)00061-3
- ¹⁶Usaj, G., Balseiro, C.A.: Transverse electron focusing in systems with spin-orbit coupling. *Phys. Rev. B* **70**, 041301 (2004). doi:10.1103/PhysRevB.70.041301
- ¹⁷Reynoso, A., Usaj, G., Balseiro, C.A.: Detection of spin polarized currents in quantum point contacts via transverse electron focusing. *Phys. Rev. B* **75**, 085321 (2007). doi:10.1103/PhysRevB.75.085321
- ¹⁸Rokhinson, L.P., Pfeiffer, L.N., West, K.W.: Spontaneous spin polarization in quantum point contacts. *Phys. Rev. Lett.* **96**, 156602 (2006). doi:10.1103/PhysRevLett.96.156602
- ¹⁹Chesi, S., Giuliani, G.F., Rokhinson, L.P., Pfeiffer, L.N., West, K.W.: Anomalous spin-resolved point-contact transmission of holes due to cubic Rashba spin-orbit coupling. *Phys. Rev. Lett.* **106**, 236601 (2011). doi:10.1103/PhysRevLett.106.236601
- ²⁰Dedigama, A.R., Deen, D., Murphy, S.Q., Goel, N., Keay, J.C., Santos, M.B., Suzuki, K., Miyashita, S., Hirayama, Y.: Current focusing in InSb heterostructures. *Physica E: Low-dimensional Systems and Nanostructures* **34**(1), 647–650 (2006). doi:10.1016/j.physe.2006.03.050
- ²¹Yan, C., Kumar, S., Thomas, K., Pepper, M., See, P., Farrer, I., Ritchie, D., Griffiths, J.P., Jones, G.A.C.: Direct observation of exchange-driven spin interactions in one-dimensional system. *Applied Physics Letters* **111**(4), 042107 (2017). doi:10.1063/1.4989374
- ²²Potok, R.M., Folk, J.A., Marcus, C.M., Umansky, V.: Detecting spin-polarized currents in ballistic nanostructures. *Phys. Rev. Lett.* **89**, 266602 (2002). doi:10.1103/PhysRevLett.89.266602
- ²³van Houten, H., Beenakker, C.W.J., Williamson, J.G., Broekaart, M.E.I., van Loosdrecht, P.H.M., van Wees, B.J., Mooij, J.E., Foxon, C.T., Harris, J.J.: Coherent electron focusing with quantum point contacts in a two-dimensional electron gas. *Phys. Rev. B* **39**, 8556–8575 (1989). doi:10.1103/PhysRevB.39.8556